Materials Transactions, JIM, Vol. 32, No. 7 (1991), 609 to 616

Mg-Cu-Y Amorphous Alloys with High Mechanical Strengths Produced by a Metallic Mold Casting Method

A. Inoue*, A. Kato*†, T. Zhang**, S. G. Kim** and T. Masumoto*

A low pressure casting of Mg-Cu-Y melts into copper molds was found to cause amorphous bulks in a cylindrical form. The maximum diameter of the amorphous cylinder (D_c) shows a significant compositional dependence and reaches a maximum value of 4.0 mm for $Mg_{65}Cu_{25}Y_{10}$. The compositional dependence of the D_c is similar to that for the temperature span of the supercooled liquid region, $\Delta T_x (= T_x - T_g)$. The similarity is presumably because the alloy with large ΔT_x has a high resistance against the nucleation and growth of a crystalline phase resulting from the formation of a disordered structure with a more dense random packing and an optimum bonding states. The compressive proof stress at an elongation of 0.2% (σ_p) for the $Mg_{80}Cu_{10}Y_{10}$ cylinder was 822 MPa at room temperature and the fracture occurred along the shear plane. The σ_p remains unchanged up to 350 K and then decreases significantly with increasing temperature, accompanied by the change in the deformation mode from inhomogeneous to homogeneous type. There is no appreciable difference in the features of mechanical strengths and deformation behavior between the bulk and ribbon samples, indicating the similarity of the disordered structure.

(Received March 25, 1991)

Keywords; *magnesium base alloy, amorphous phase, cylindrical sample, metallic mold casting, supercooled liquid region, high glass-forming capacity, high proof stress*

I. Introduction

It has recently been reported that light-metal base alloys containing Al[1] or Mg[2][3] as a main component can be amorphized in very wide composition ranges by the melt spinning technique and their amorphous alloys exhibit high specific mechanical strengths and good ductility. In addition, Mg-based amorphous alloys in Mg-Ni-Ln and Mg-Cu-Ln (Ln=lanthanide metal) systems have been found[4][5] to have a wide supercooled liquid region reaching about 70 K before crystallization. The appearance of the extremely wide supercooled liquid region indicates that the thermal stability of the supercooled liquid in their Mg-based systems is very high and the nucleation and growth of a crystalline phase is significantly suppressed probably because of a unique disordered structure at their alloy compositions. The large difficulty of nucleation and growth of a crystalline phase allows us to expect that their Mg-based alloys have an extremely large glass-forming capacity and an amorphous single phase in a bulk form is formed by casting their molten alloys into a copper mold. The trial of producing Mg-based amorphous bulks by the metallic mold casting method is expected to cause a new type of light-metal alloys with high mechanical strengths. This paper is intended to examine the possibility of formation of an amorphous bulk and its maximum sample thickness in a Mg-Cu-Y system by the metallic mold casting method and to clarify the thermal stability and mechanical strengths of the resultant amorphous bulk, in comparison with the previous data[3] on melt-spun amorphous Mg-Cu-Y ribbons.

* Institute for Materials Research, Tohoku University, Sendai 980, Japan.
** Graduate Student, Tohoku University, Sendai.
† On leave from Higashifuji Technical Center, Toyota Motor Co., Susono 410-11, Japan.

II. Experimental Procedure

Ternary Mg-Cu-Y alloys were used in the present study because their alloys had the widest supercooled liquid region in Mg-based alloy systems. Their ingots were prepared by induction-melting a mixture of pure Mg (99.99 mass%), Cu (99.99 mass%) and Y (99.99 mass%) metals in a purified argon atmosphere. The compositions are nominally expressed in atomic per cent hereafter. From the master alloy ingots, cylindrical samples with a constant length of 50 mm and different diameters of 1.0 to 7.0 mm were prepared by injection casting of the melt into copper molds with an inner shape of cylinder. The injection pressure was fixed to be 0.30 MPa. For comparison, an amorphous ribbon with a cross section of about 0.02×1 mm^2 was also produced by the single roller melt spinning method in an argon atmosphere.

The amorphicity of the as-cast samples in the cylinder form was examined by X-ray diffractometry and optical microscopy techniques. The specific heat (C_p) associated with structural relaxation, glass transition and crystallization was measured at a heating rate of 0.67 K/s (40 K/min) with a differential scanning calorimeter (DSC). Hardness was measured at room temperature by a Vickers microhardness tester with a 4.9 N (500 gf) load. Compressive strength of the cylinder specimens and tensile strength of the ribbon specimens were measured in

the temperature range of 293 to 443 K by an Instron-type tensile testing machine at a strain rate of $6.2 \times 10^{-4}\ s^{-1}$. The testing temperature was controlled by using a heating medium of silicon oil. Compressive specimens were machined from the cast cylinder into cylinders having a dimension of 1.35 mm in diameter and 2.70 mm in height and tensile specimens were cut from the melt-spun ribbon into strips having a gauge dimension of 20 mm long. Subsequent to compressive and tensile testings, the fracture surface appearance was examined by optical or scanning electron microscopy. The melting temperature of the as-cast ingots and melt-spun ribbons was measured at a scanning rate of 0.33 K/s (20 K/min) with a differential thermal analyzer (DTA).

III. Results

Figure 1 shows the surface appearance of the as-cast $Mg_{80}Cu_{10}Y_{10}$ cylinder with a diameter of 1.5 mm. The length of the sample is fixed to be 50 mm from the inner shape of the copper mold. As shown in the photograph, neither holes nor cavities are seen on the outer surface of the as-cast sample and the surface has a good luster. Considering that the shape and dimension of the as-cast sample are just the same as the inner shape of the copper mold, the metallic mold pressure casting method seems to be useful for the production of the Mg–Cu–Y bulk samples with various shapes and dimensions.

Figure 2 shows the X-ray diffraction patterns of the as-cast $Mg_{80}Cu_{10}Y_{10}$ cylinders with different diameters of 1.0 and 1.5 mm, along with the result of a melt-spun Mg–Cu–Y ribbon with the same composition. The cylinders as well as the ribbon have a broad diffraction peak at $K_p = 25.54\ nm^{-1}$ and no diffraction peak corresponding to a crystalline phase is seen even in the former bulk samples, indicating that a mostly single amorphous phase is formed by the casting method. No appreciable difference in the K_p value is observed among the three samples in cylinder and ribbon forms. The agreement indicates that there is no significant change in the amorphicity of the Mg–Cu–Y samples prepared by casting and melt spinning, in spite of the large difference in cooling rate of the melt. It is therefore reasonable to conclude that the $Mg_{80}Cu_{10}Y_{10}$ alloy has the glass-forming capacity enough to produce an amorphous single phase even by the casting method.

Figure 3 shows an optical micrograph revealing a transverse cross-sectional surface of the as-cast $Mg_{80}Cu_{10}Y_{10}$ cylinder with a diameter of 1.5 mm. Even after an etched state for 30 s at room temperature in

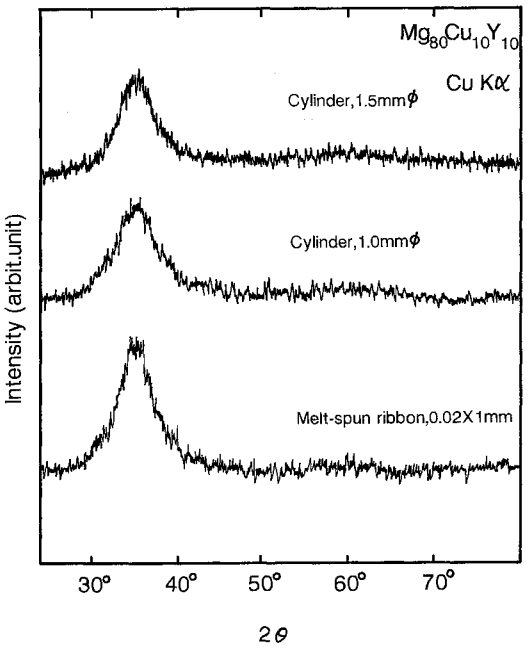

Fig. 2 X-ray diffraction patterns of a $Mg_{80}Cu_{10}Y_{10}$ alloy in a cylindrical form produced by low pressure casting into copper molds. The data on a melt-spun $Mg_{80}Cu_{10}Y_{10}$ ribbon are also shown for comparison.

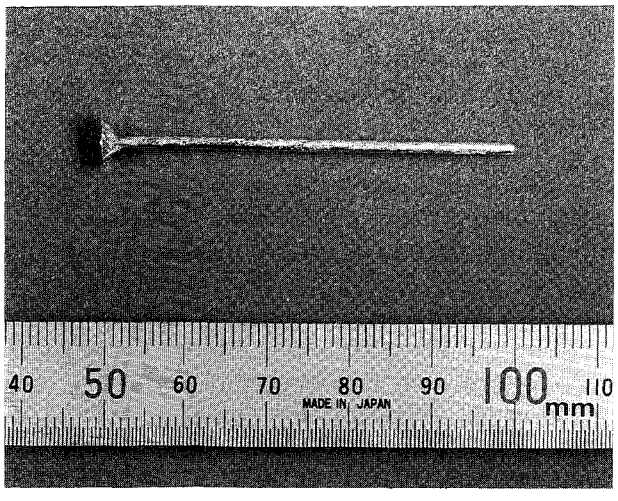

Fig. 1 Surface appearance of a $Mg_{80}Cu_{10}Y_{10}$ alloy in a cylindrical form produced by low pressure casting into a copper mold.

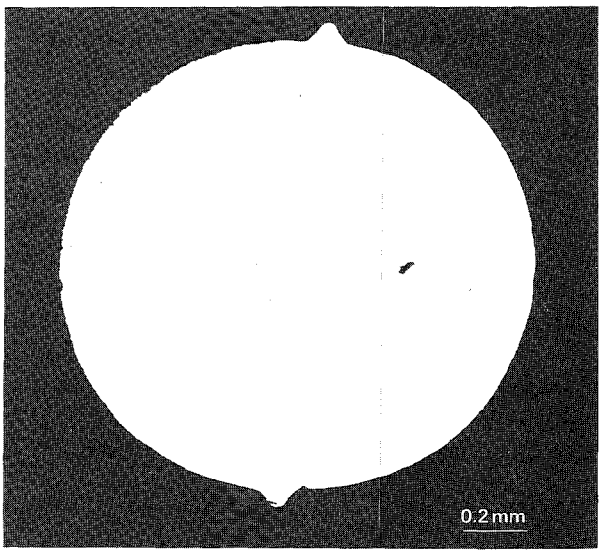

Fig. 3 Optical micrograph of the transverse cross-section in a $Mg_{80}Cu_{10}Y_{10}$ cylinder produced by low pressure casting into a copper mold.

an aqueous solution of 1% NaCl, no contrast corresponding to the precipitation of any crystalline phases is seen over the entire transverse cross section. Thus, the cylindrical sample is composed of an amorphous phase which does not include any appreciable crystalline phase, in agreement with the result obtained by X-ray diffractometry. In addition, the sample has an approximately circular cross-section, though burrs resulting from the use of a split-type mold are seen on the outer surface.

The DSC curves of the amorphous $Mg_{80}Cu_{10}Y_{10}$ cylinders are shown in Fig. 4, along with that of the melt-spun amorphous ribbon. The T_g and T_x of the bulk samples are 427 and 448 K, respectively, independent of the diameter of the cylinders. Furthermore, there is no appreciable difference in the T_g and T_x values between the cast and melt-spun samples. The heat of crystallization (ΔH_x) was measured to be 1.55 to 1.61 kJ/mol for the cylinders with diameters of 1.0 and 1.5 mm and 1.59 kJ/mol for the ribbon, being nearly the same in the three samples. It is thus concluded that the sequent transition behavior of glass transition, supercooled liquid and crystallization is independent of the preparation conditions. However, there is an appreciable difference in the DSC curves at temperatures below T_g between the cast and melt-spun samples as shown in Fig. 4, suggesting that the heat of irreversible structural relaxation has a significant difference in both states because of a large difference in cooling rate.

In order to clarify the difference in the irreversible structural relaxation behavior between the bulk and ribbon samples, Fig. 5 shows the thermograms of the amorphous $Mg_{80}Cu_{10}Y_{10}$ cylinders with different diameters of 1.0 and 1.5 mm produced by casting, along with those of the melt-spun amorphous ribbon. Similar thermograms are seen in the three samples. As the temperature rises, the C_p value of the amorphous bulks increases gradually and begins to decrease, indicating an irreversible structural relaxation at 377 K (T_r) for the 1.0 mm$^{\phi}$ cylinder and 382 K for the 1.5 mm$^{\phi}$ cylinder. With a further increase in temperature, the C_p value shows its minimum in the temperature range of 395 to 403 K, then increases rapidly in the glass transition range from 427 to 448 K and reaches 35.4 J/mol·K for the supercooled liquid around 437 K. Above this temperature, the supercooled liquid crystallizes at 448 K, accompanied by ΔH_x of about 1.6 kJ/mol as described in Fig. 4. It is also seen in Fig. 5 that the cast samples have a large difference, $\Delta C_{p,s\to l}$ in specific heat between the reheated amorphous solid and supercooled liquid reaching about 8.8 J/mol·K. The difference in $C_p(T)$ between the as-quenched and the reheated states, $[\Delta C_p(T)]$, manifests the irreversible structural relaxation which is presumed to arise from the annihilation of quenched-in "defects" and the enhancement of the topological and chemical short-range ordering through the atomic rearrangement. The heat of the irreversible structural relaxation, $\Delta H_r(\equiv \int \Delta C_p \, dT$, $\Delta C_p = C_{p,s} - C_{p,q} \geq 0)$, was evaluated to be 178 J/mol for the cylinder with 1.0 mm in diameter, 75 J/mol for the cylinder with 1.5 mm in diameter and 260 J/mol for the ribbon. Comparing the thermograms of the cast samples with those of the melt-spun ribbon, it is to be noticed that the former samples have higher values by 6 to 11 K for T_r and smaller values by 82 to 185 J/mol for ΔH_r and there are no significant differences in T_g, $\Delta C_{p,s\to l}$, T_x and

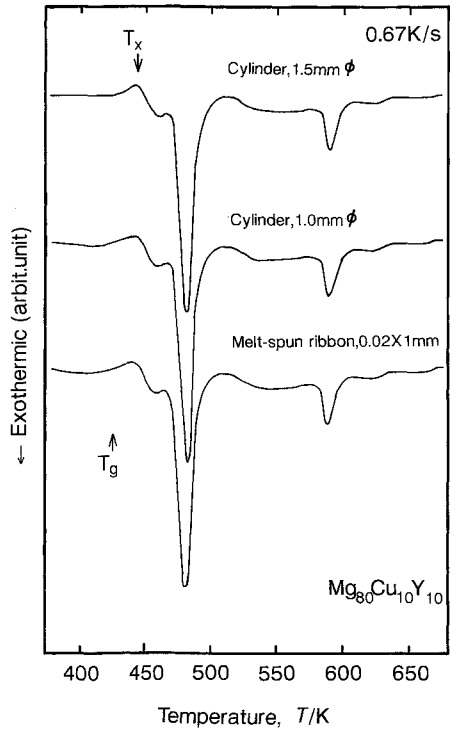

Fig. 4 Differential scanning calorimetric (DSC) curve of amorphous $Mg_{80}Cu_{10}Y_{10}$ cylinders with diameters of 1.0 and 1.5 mm. The data on a melt-spun amorphous $Mg_{80}Cu_{10}Y_{10}$ ribbon are also shown for comparison.

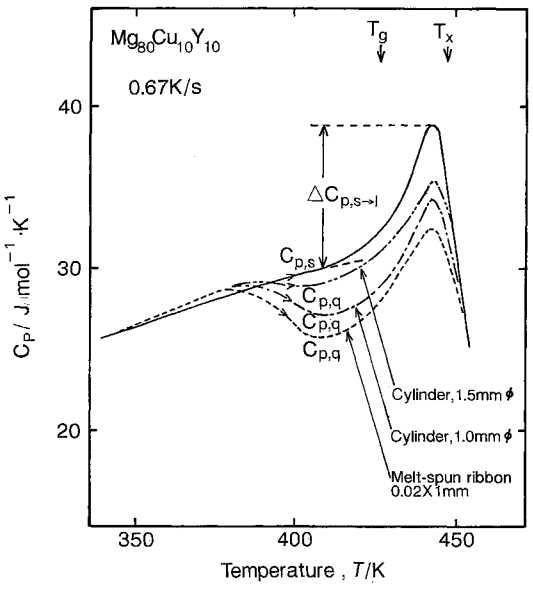

Fig. 5 The thermogram $C_{p,q}(T)$ in the as-quenched state for amorphous $Mg_{80}Cu_{10}Y_{10}$ cylinders with diameters of 1.0 and 1.5 mm. The solid line represents the thermogram $C_{p,s}(T)$ of the samples heated up to 420 K. The data on a melt-spun amorphous $Mg_{80}Cu_{10}Y_{10}$ ribbon are also shown for comparison.

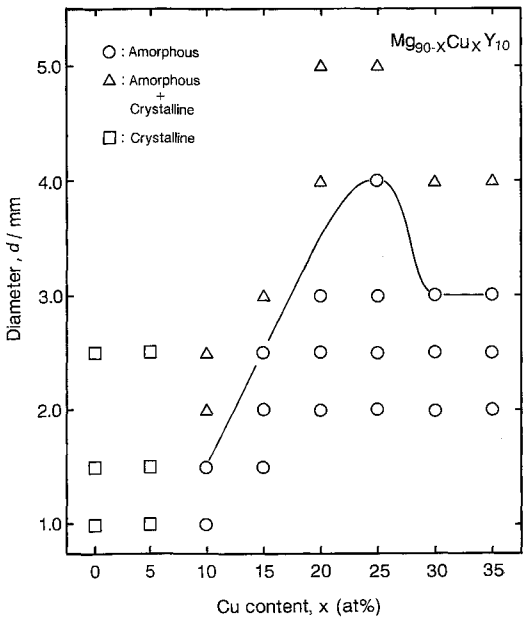

Fig. 6 Change in the maximum diameter for formation of an amorphous cylinder in $Mg_{90-x}Cu_xY_{10}$ ($x \leq 35$ at%) alloys by low pressure casting into copper molds as a function of Cu content.

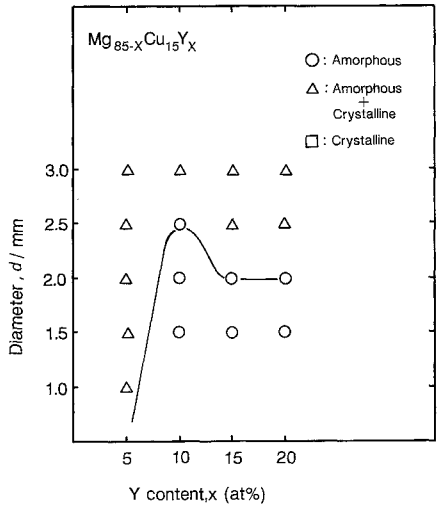

Fig. 7 Change in the maximum diameter for formation of an amorphous cylinder in $Mg_{85-x}Cu_{15}Y_x$ ($x \leq 20$ at%) alloys by low pressure casting into copper molds as a function of Y content.

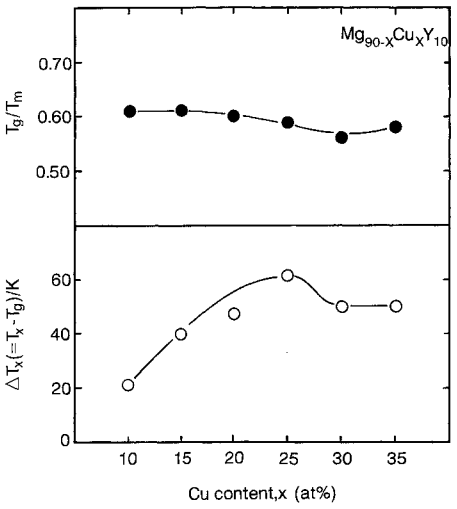

Fig. 8 Changes in T_g/T_m and $\Delta T_x(=T_x-T_g)$ of amorphous $Mg_{90-x}Cu_xY_{10}$ cylinders with a constant diameter of 2.0 mm produced by low pressure casting into a copper mold as a function of Cu content.

ΔH_x. The smaller ΔH_r values for the cast samples imply that the amorphous phase produced by casting has a more relaxed atomic configuration as compared with that for the melt-spun amorphous phase because of the lower cooling rate. Furthermore, it is seen in Fig. 5 that the cylinder with 1.0 mm in diameter has a lower T_r and a larger ΔH_r as compared with those for the cylinder with 1.5 mm in diameter, even though no appreciable difference is seen in the T_g and ΔH_x.

The compositional dependence of the critical diameter for formation of a mostly single amorphous cylinder was examined for $Mg_{90-x}Cu_xY_{10}$ and $Mg_{85-x}Cu_{15}Y_x$ alloys. Figures 6 and 7 show the plots of the critical diameter as a function of Cu or Y content, respectively. The critical diameter of the $Mg_{90-x}Cu_xY_{10}$ alloys increases significantly from 1.5 mm at 10 %Cu to 4.0 mm at 25%Cu and then decreases to 3.0 mm at 35%Cu. Similarly, the $Mg_{85-x}Cu_{15}Y_x$ alloys have a maximum diameter of 2.5 mm at 10%Y. These data indicate clearly the existences of a significant alloy composition dependence of the glass-forming capacity and an optimum alloy composition at which an amorphous bulk sample with the largest cross section is obtained.

In order to look for a dominant factor for the compositional dependence of the critical diameter for Mg-Cu-Y alloys, the $\Delta T_x(=T_x-T_g)$ value as well as the T_g/T_m value which has generally been regarded[6] as dominant factors for the glass-forming capacity is plotted as a function of Cu content for the $Mg_{90-x}Cu_xY_{10}$ cylinders with a diameter of 1.5 mm in Fig. 8 and as a function of Y content for the $Mg_{85-x}Cu_{15}Y_x$ cylinders with a diameter of 1.5 mm in Fig. 9. Although the T_g/T_m value remains almost constant (0.60) in the entire Cu and Y concentration ranges, the ΔT_x value has a clear compositional dependence and shows a maximum value at 25%Cu for the $Mg_{90-x}Cu_xY_{10}$ alloys and at 10%Y for the $Mg_{85-x}Cu_{15}Y_x$ alloys. The contrast result in the compositional dependences for T_g/T_m and ΔT_x indicates clearly that the compositional dependence of the critical diameter for formation of an amorphous cylinder is mainly dominated by the ΔT_x value.

Mechanical properties

Figure 10 shows the nominal compressive stress and elongation curves of the $Mg_{80}Cu_{10}Y_{10}$ amorphous cylinder tested at different temperatures between 293 and 443 K. The feature of the stress-elongation curve can be divided into the following three types. That is, (1) high yield stress and small elongation in the temperature range below about 355 K, (2) a clear yield phenomenon, follow-

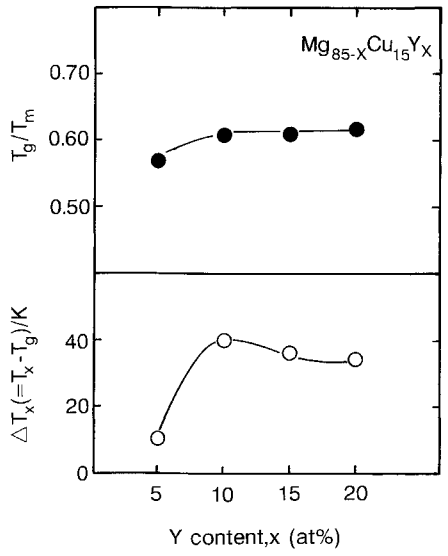

Fig. 9 Changes in T_g/T_m and $\Delta T_x(=T_x-T_g)$ of amorphous $Mg_{85-x}Cu_{15}Y_x$ cylinders with a constant diameter of 2.0 mm produced by low pressure casting into a copper mold as a function of Y content.

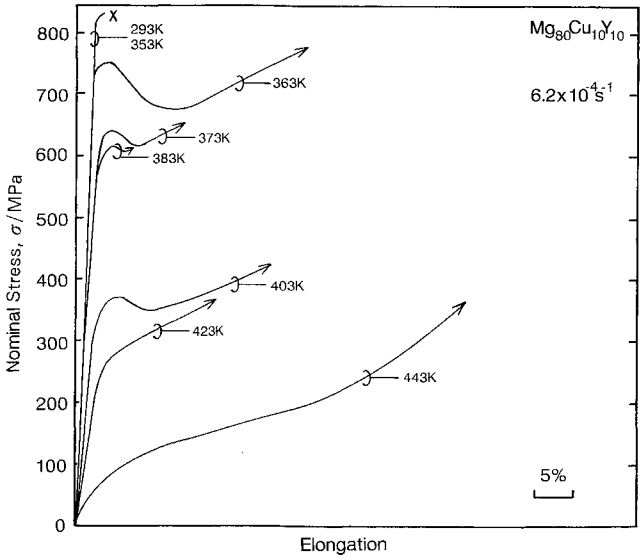

Fig. 10 Nominal stress-elongation curves of an amorphous $Mg_{80}Cu_{10}Y_{10}$ cylinder subjected to a compressive testing at temperatures ranging from 293 to 443 K.

ed by a significant decrease and an increase in nominal flow stress in the range of about 360 to 410 K, and (3) a gradual increase in flow stress after yielding in the range above about 410 K. On the basis of the nominal stress-elongation curves shown in Fig. 10, the proof stress at a fixed elongation of 0.2% is plotted as a function of temperature in Fig. 11. The proof stress is 822 MPa at room temperature, remains almost unchanged at temperatures up to 350 K and then decreases rapidly with increasing temperature. Thus, the high proof stress exceeding 550 MPa is kept in the temperature range below 373 K. It is notable that the proof stresses at temperatures below 373 K are about two to three times as high as the highest

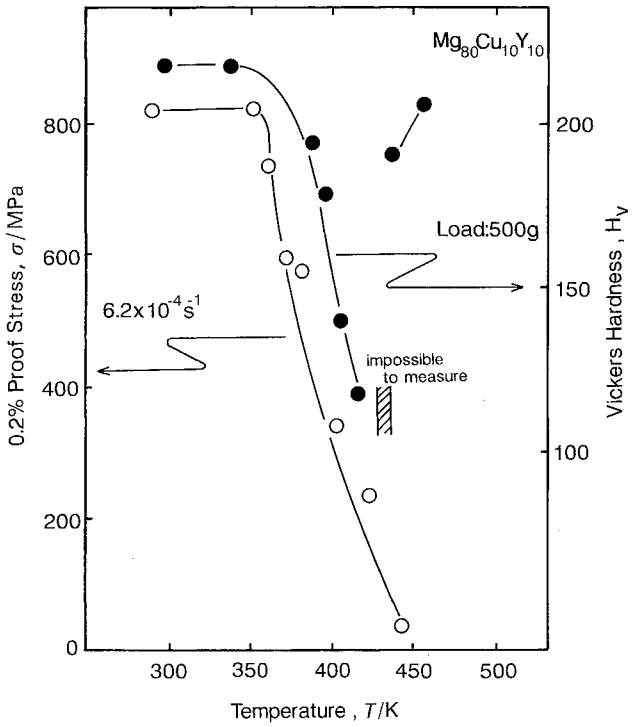

Fig. 11 Change in the 0.2% proof stress and Vickers hardness (H_v) of an amorphous $Mg_{80}Cu_{10}Y_{10}$ cylinder with testing temperature.

value[7] of conventional Mg-based crystalline alloys.

The temperature dependence similar to that for the proof stress of the bulk samples was also obtained for the Vickers hardness. As shown in Fig. 11, the H_v value of the amorphous $Mg_{80}Cu_{10}Y_{10}$ cylinder with a diameter of 1.5 mm also keeps a constant value of 220 in the temperature range up to 373 K, and decreases rapidly to 118 at 413 K. In the supercooled liquid region between 427 to 448 K, the sample is too soft to give an indentation trace by a Vickers diamond indenter. With further increasing temperature, the H_v value increases remarkably through the transition of amorphous to crystalline phase.

In order to clarify the reason for the distinction of the deformation behavior into the three types, the fracture

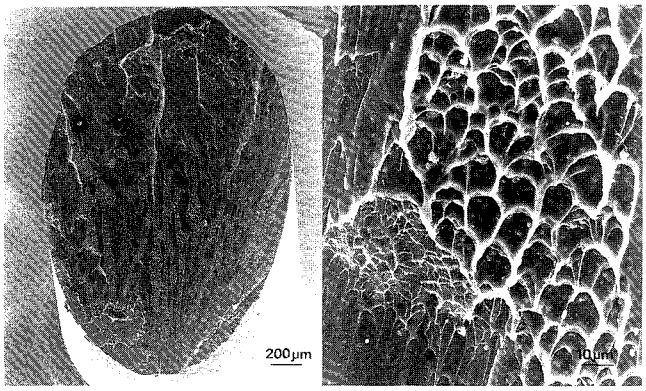

Fig. 12 Scanning electron micrographs recealing the fracture surface appearance of an amorphous $Mg_{80}Cu_{10}Y_{10}$ cylinder.

surface appearance of the cylinder samples was examined by SEM. The SEM shown in Fig. 12(a) and (b) reveal the whole fracture surface appearance of the $Mg_{80}Cu_{10}Y_{10}$ amorphous cylinder fractured at room temperature and the enlarged pattern on the fracture surface, respectively. One can see that the fracture occurs along the shear plane declined by 45 to 55 degrees to the longitudinal direction parallel to the applied direction of compressive stress and the fracture surface consists mostly of a vein pattern which has been thought[8] to generate during the final rupture. The typical shear-type fracture and the appearance of the clear vein pattern indicate that the amorphous bulk sample has a good ductility inherent to an amorphous phase produced by various rapid solidification techniques from melts and the final rupture takes place after a small amount of shear sliding. The shear sliding is also confirmed from the data on the stress-elongation curves shown in Fig. 10, where a plastic elongation of about 1.0% is observed. On the basis of the deformation-fracture behavior for the cylindrical sample at room temperature, one can presume the origin for the appearance of the nominal stress-elongation curves belonging to the type II. The inhomogeneous deformation which occurs through the sliding on the shear plane results in a decrease in the true cross sectional area, leading to the decrease in the nominal flow stress. However, the limitation of the sliding deformation to the shear plane is not always strict at elevated temperatures between 360 and 403 K in the transient range from inhomogeneous to homogeneous deformation mode. Accordingly, the coexistence of inhomogeneous and homogeneous deformations which is presumed to occur immediately after the shear sliding suppresses the progress of the final fracture, resulting in an increase in nominal flow stress resulting from an increase of cross sectional area caused by the deformation of the cylindrical sample to the barrel shape. In the high temperature range above about 410 K, the sample is deformed homogeneously through a viscous flow mechanism in the entire elongation range, resulting in a disappearance of the maximum phenomenon of the nominal flow stress. The above-described presumption on the reason for the appearance of the maximum phenomenon of nominal flow stress is also supported from the result that the shape of the maximum peak is dependent on testing temperature in the entire temperature range belonging to the type II.

Table 1 summarizes the compressive proof stress and Vickers hardness of the amorphous $Mg_{80}Cu_{10}Y_{10}$ cylinder produced by the metallic mold casting method, along with the tensile fracture strength and hardness of the melt-spun amorphous Mg–Cu–Y ribbon with the same alloy composition. In addition to nearly the same hardness values between the cylindrical and ribbon samples, it is notable that the compressive proof stress of the cylindrical sample is also nearly the same as the tensile fracture strength of the melt-spun ribbon. These mechanical strengths also suggest that there is no significant difference in the disordered structure in spite of the large difference in cooling rate between the bulk and ribbon samples.

Table 1 Mechanical properties of an amorphous $Mg_{80}Cu_{10}Y_{10}$ cylinder produced by the metallic mold casting method. The data on a melt-spun amorphous $Mg_{80}Cu_{10}Y_{10}$ ribbon are also shown for comparison.

Method	Shape	$\sigma_p^{(1)}$, $\sigma_f^{(2)}$ (MPa)	H_v
Metallic mold casting	Cylinder 1.5 mm$^{\phi}$	822[1]	220
Melt spinning	Ribbon 0.02 × 1 mm	820[2]	218

Compressive proof stress at an elongation of 0.2% (σ_p), tensile fracture strength (σ_f) and Vickers hardness (H_v).

IV. Discussion

It is shown in section III that the metallic mold casting method causes amorphous Mg–Cu–Y bulk samples with the same thermal stability and mechanical strengths as those for the melt-spun amorphous ribbon samples produced by melt spinning, even though the heat of irreversible structural relaxation is considerably smaller for the bulk samples. These results indicate that the glass-forming capacity of the Mg–Cu–Y alloys is large enough to cause an amorphous single phase even at small cooling rates obtained by the metallic mold casting method. Recently, Ono *et al.*[9] have evaluated the cooling rate as a function of diameter during casting of the $Mg_{65}Cu_{25}Y_{10}$ molten alloy into copper molds by using the finite difference equations which were derived based on the direct finite difference method[10]. The evaluation was made in the assumption that (1) the mold cavity is instantaneously filled with a melt, (2) the temperature in the melt is uniform, and (3) the flow during pouring is neglected. In addition, in the calculation, they used the measured values of density (3.13 Mg/m^3), specific heat (712 J/kg·K), melting temperature (713 K) and the temperature of melt just before pouring (883 K) for $Mg_{65}Cu_{25}Y_{10}$ and the reference values[7] of thermal conductivity of pure magnesium (167 W/m·K) and copper (393 W/m·K) and density (8.93 Mg/m^3) and specific heat (389 J/kg·K) of pure copper. Furthermore, the heat transfer coefficient (h) used in the evaluation was 586 W/m^2·K which had actually been measured[9] between $Mg_{65}Cu_{25}Y_{10}$ and copper mold. The relation between cooling rate and diameter of the cylinder thus evaluated[9] is shown in Fig. 13. The cooling rate of the cylinders with diameters ranging from 1.0 to 4.0 mm lies in the range of 391 to 93 K/s, indicating that the amorphous cylinders were produced at the very small cooling rates. On the basis of the data shown in Figs. 6, 7 and 13 and the assumption that the evaluation of the above-described cooling rate is also valid for other Mg–Cu–Y alloys, the critical cooling rate for formation of the amorphous cylinder by the metallic mold casting method is plotted as a function of Cu or Y content for the $Mg_{90-x}Cu_xY_{10}$ and $Mg_{85-x}Cu_{15}Y_x$ alloys in Fig. 14. One can notice that the

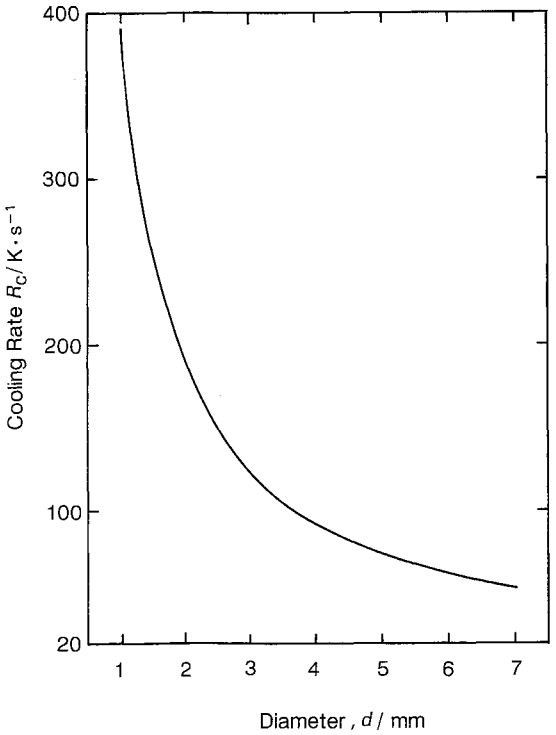

Fig. 13 Change in the cooling rate evaluated by the direct finite difference method during casting of a $Mg_{65}Cu_{25}Y_{10}$ alloy into a copper mold as a function of diameter.

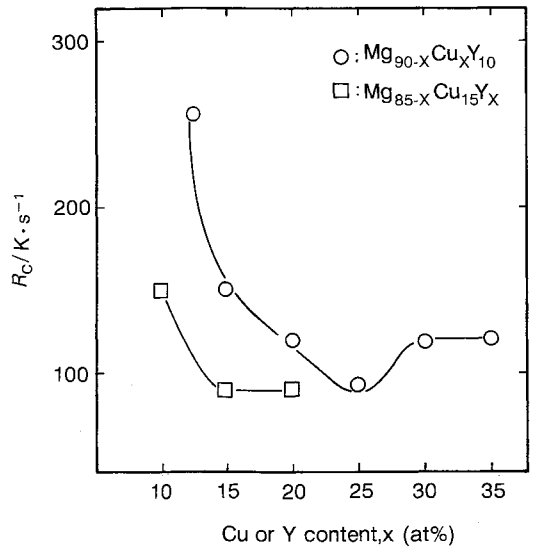

Fig. 14 Change in the critical cooling rate for formation of an amorphous cylinder (R_c) by the metallic mold casting method as a function of Cu or Y content for $Mg_{90-x}Cu_xY_{10}$ and $Mg_{85-x}Cu_{15}Y_x$ alloys.

critical cooling rate for formation of the amorphous cylinder shows a minimum value of 93 K/s at 25%Cu and 159 K/s at 10%Y. Furthermore, from the comparison of Fig. 14 with Figs. 8 and 9, the critical cooling rate appears to be closely related to the $\Delta T_x(=T_x-T_g)$ value. Figure 15 shows the relation between the ΔT_x value and the critical cooling rate (R_c) for the Mg-Cu-Y amorphous alloys. There exists a clear tendency that the larger

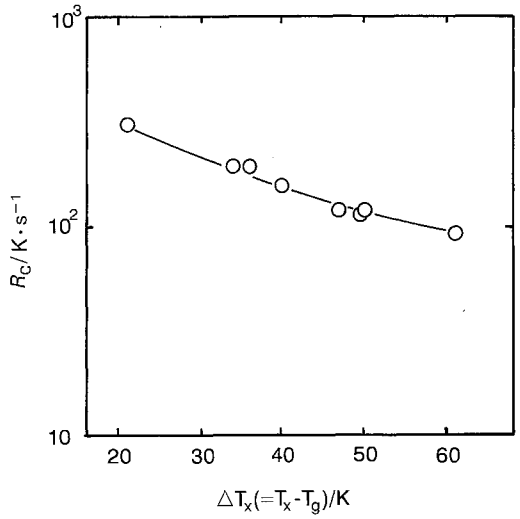

Fig. 15 Relation between the critical cooling rate for formation of an amorphous cylinder by the metallic mold casting method and the temperature span between T_g and T_x, $\Delta T_x(=T_x-T_g)$ for Mg-Cu-Y amorphous alloys.

the ΔT_x value the smaller is the Rc. In addition, the result shown in Fig. 15 is believed to be the first evidence in which the ΔT_x value has a close relation to the glass-forming capacity for amorphous metallic materials. The clear tendency allows us to have the following concept; the high thermal stability of the supercooled liquid which is evidenced for the large ΔT_x value implies that the liquid supercooled to a temperature below melting temperature also has a high resistance to the transition to a crystalline phase during cooling, leading to a small R_c. Thus, the small R_c values for the Mg-Cu-Y alloys are concluded to result from a disordered structure leading to the wide suprcooled liquid region.

Subsequently, we shall discuss the reason for the high resistance of the supercooled liquid against the nucleation and growth of a crystalline phase in the Mg-Cu-Y system. Since the short-range ordered structure of an amorphous alloy has been pointed out to reflect the structure of equilibrium compounds[11], an equilibrium phase of $Mg_{80}Cu_{10}Y_{10}$ and $Mg_{65}Cu_{25}Y_{10}$ alloys was examined by conventional metallographic techniques. As a result, the equilibrium structure was identified to consist of mixed phases of Mg, $Mg_{24}Y_5$ and Mg_2Cu for the former alloy and Mg_2Y, Mg_2Cu and Cu_3Y for the latter alloy. In addition, the atomic radii of the constituent Mg, Cu and Y elements are 0.160, 0.128 and 0.182 nm, respectively, and hence the atomic size ratio against Mg is as large as 0.80 for Cu and 1.14 for Y. That is, the Mg-Cu-Y amorphous alloys are composed of the three elements with a larger size (Y), a medium size (Mg) and a smaller size (Cu). In spite of the large atomic size ratios, the three kinds of atoms are thought to mix homogeneously in the amorphous solid and the supercooled liquid. Furthermore, the large difference of the atomic sizes is thought to lead to the construction of a more dense random packing structure. When the homogeneously mixed amorphous phase crystallizes to the $Mg+Mg_{24}Y_5+Mg_2Cu$ for

the $Mg_{80}Cu_{10}Y_{10}$ and the $Mg_2Cu+Mg_2Y+Cu_3Y$ for the $Mg_{65}Cu_{25}Y_{10}$, the constituent elements must be redistributed over a long-range scale, implying the necessity of a long-range diffusion of the constituent atoms. The long-range diffusion is believed to be more difficult for an amorphous alloy with a more dense random packing structure. The necessity and difficulty of the long-range diffusion cause the retardation of nucleation and growth of their equilibrium compounds in the amorphous solid and supercooled liquid, leading to the appearance of the wide supercooled liquid region before crystallization as well as the large glass-forming capacity (the small critical cooling rate for formation of an amorphous phase).

V. Summary

It was found that an amorphous bulk in a cylindrical form in Mg–Cu–Y system is produced by casting the melt into a copper mold. The critical diameter for formation of an amorphous phase (D_c) is in the range of 1.0 to 4.0 mm in the composition range of 10 to 35%Cu and 10 to 20%Y and shows the maximum value for $Mg_{65}Cu_{25}Y_{10}$. There is no appreciable difference in the glass transition temperature (T_g) and the onset temperature of crystallization (T_x) between the amorphous cylinder with 1.5 mm in diameter and the melt-spun amorphous ribbon with 0.02 mm in thickness, while the onset temperature of structural relaxation (T_r) is higher and the heat of structural relaxation (ΔH_x) is smaller for the amorphous cylinder because of a more relaxed disordered structure in the amorphous cylinder. Although the critical diameter for formation of an amorphous cylinder is independent of the reduced glass transition temperature (T_g/T_m), it has a close relation to the temperature span between T_g and T_x, $\Delta T_x(=T_x-T_g)$ and there is a clear tendency that the larger the ΔT_x the larger is the D_c. In addition, on the basis of the cooling rates as a function of diameter for the $Mg_{65}Cu_{25}Y_{10}$ cylinder in the metallic mold casting which were evaluated by the direct finite difference method, we examined the compositional dependence of the critical cooling rate for formation of the amorphous Mg–Cu–Y cylinders. The critical cooling rate lies in the range from 93 to 391 K/s and has a minimum value for $Mg_{65}Cu_{25}Y_{10}$ with the largest ΔT_x. The good agreement between D_c (or R_c) and ΔT_x indicates that the alloy with the wide supercooled liquid region also has a high resistance against the nucleation and growth of a crystalline phase probably because of the formation of a more dense random packing structure consisting of the three kinds of atoms with attractive interactions and large atomic size ratios.

The compressive proof stress at an elongation of 0.2% (σ_p) for the amorphous $Mg_{80}Cu_{10}Y_{10}$ cylinder is 822 MPa in the temperature range below 350 K and decreases significantly with increasing temperature, accompanied by the change in the deformation mode from inhomogeneous to homogeneous type at about 360 K. The σ_p at room temperature is nearly the same as the tensile fracture strength for the melt-spun ribbon, indicating the formation of a similar disordered structure in spite of the significant difference in cooling rate.

Acknowledgement

The authors are grateful to the Ministry of Education, Culture and Science for support of the present cooperative research between Tohoku University and Toyota Motor Co.

REFERENCES

(1) A. Inoue and T. Masumoto: Bulletin Japan Inst. Metals, **28** (1989), 968.
(2) A. Inoue, K. Ohtera, K. Kita and T. Masumoto: Jpn. J. Appl. Phys., **27** (1988), L2248.
(3) S. G. Kim, A. Inoue and T. Masumoto: Mater. Trans., JIM, **31** (1990), 929.
(4) A. Inoue, M. Kohinata, A. P. Tsai and T. Masumoto: Mater. Trans., JIM, **30** (1989), 378.
(5) A. Inoue, K. Ohtera, M. Kohinata, A. P. Tsai and T. Masumoto: J. Non-cryst. Solids, **117/118** (1990), 712.
(6) H. A. Davies: *Amorphous Metallic Alloys*, ed. by F. E. Luborsky, Butterworths, London, (1983), p. 8.
(7) *Metals Databook*, Japan Inst. Metals, Maruzen, Tokyo (1983).
(8) H. S. Chen: Rep. Prog. Phys., **3** (1980), 353.
(9) T. Ono, Y. Otsuka, and A. Kato: Toyota Motor Co., private communication, 1990.
(10) I. Ohnaka and T. Fukusako: Trans. ISIJ, **21** (1981), 485.
(11) K. Suzuki: *Materials Science of Amorphous Metals*, ed. by T. Masumoto, Ohmu Publishing Co., Tokyo, (1982), p. 48.